Protein Science (1996), 5:1081-1092. Cambridge University Press. Printed in the USA.

The heme redox center of chloroplast cytochrome *f* is linked to a buried five-water chain

S.E. MARTINEZ,[1] D. HUANG, M. PONOMAREV, W.A. CRAMER, AND J.L. SMITH
Department of Biological Sciences, Purdue University, West Lafayette, Indiana 47907

(RECEIVED December 27, 1995; ACCEPTED March 28, 1996)

Abstract

The crystal structure of the 252-residue lumen-side domain of reduced cytochrome *f*, a subunit of the proton-pumping integral cytochrome b_6f complex of oxygenic photosynthetic membranes, was determined to a resolution of 1.96 Å from crystals cooled to −35°. The model was refined to an *R*-factor of 15.8% with a 0.013-Å RMS deviation of bond lengths from ideality. Compared to the structure of cytochrome *f* at 20°, the structure at −35° has a small change in relative orientation of the two folding domains and significantly lower isotropic temperature factors for protein atoms. The structure revealed an L-shaped array of five buried water molecules that extend in two directions from the Nδ1 of the heme ligand His 25. The longer branch extends 11 Å within the large domain, toward Lys 66 in the prominent basic patch at the top of the large domain, which has been implicated in the interaction with the electron acceptor, plastocyanin. The water sites are highly occupied, and their temperature factors are comparable to those of protein atoms. Virtually all residues that form hydrogen bonds with the water chain are invariant among 13 known cytochrome *f* sequences. The water chain has many features that optimize it as a proton wire, including insulation from the protein medium. It is suggested that this chain may function as the lumen-side exit port for proton translocation by the cytochrome b_6f complex.

Keywords: cytochrome b_6f complex; electron transfer; energy transduction; heme protein; proton translocation

The cytochrome b_6f integral membrane protein complex transfers electrons between the two reaction center complexes of oxygenic photosynthetic membranes, and participates in formation of the *trans*-membrane electrochemical proton gradient by also transferring protons from the stromal (electrochemically negative, **n**) to the internal lumen (electrochemically positive, **p**) compartment (Cramer et al., 1994a). The cytochrome b_6f complex contains four polypeptides of molecular weight greater than 15,000, of which three contain redox prosthetic groups [cytochrome *f* (285 residues), cytochrome b_6 (215 residues), and the Rieske iron-sulfur protein (179 residues)], three are organelle-encoded [cytochrome *f*, cytochrome b_6, and subunit IV (160 residues)], and three have highly conserved amino acid sequences (Cramer et al., 1994b). In its structure and functions, the cytochrome b_6f complex bears extensive analogy to the cytochrome bc_1 complex of mitochondria and photosynthetic purple bacteria.

Proton transfer to the lumen compartment of the thylakoid membrane is linked to the oxidation of plastoquinol by the Rieske iron-sulfur protein near the lumen-side membrane interface (Malkin, 1982). However, there is no structural information on the nature of the intraprotein pathway of proton transfer from this oxidation site to the terminal proton deposition in the aqueous phase.

Relatively little is known about structural aspects of pathways of *trans*-membrane proton translocation in any energy-transducing membrane. The two systems where discrete amino acids have been shown to have a role in the proton translocation mechanism are bacteriorhodopsin of the halophilic purple bacteria (Henderson et al., 1990; Cao et al., 1991; Lanyi, 1993), and the photosynthetic reaction center of the purple bacteria (Paddock et al., 1989; Takahashi & Wraight, 1990). Structural features that are common to bacteriorhodopsin and the reaction center are intramembrane carboxylate residues with unusually high p*K* values (pK_a 9) and water molecules in or near the pathway of proton trans-location.

This manuscript is dedicated to Prof. D.W. Krogmann on the occasion of his 65th birthday.

Reprint requests to: W.A. Cramer or J.L. Smith, Department of Biological Sciences, Purdue University, West Lafayette, Indiana 47907.

[1] Present address: Department of Pharmacology, SJ-30, University of Washington, Seattle, Washington 98195.

Abbreviations: CAPS, 3-[cyclohexylamino]-1-propanesulfonic acid; E_m, midpoint redox potential; HEPES, *N*-[2-hydroxyethyl]piperazine-*N'*-[2-ethanesulfonic acid]; MES, 2-[*N*-morpholino]ethanesulfonic acid; MOPS, 3-[*N*-morpholino]propanesulfonic acid.

Proton uptake is associated with reduction of the secondary quinone (Q_B) in the photosynthetic reaction center of the purple bacteria. An ordered chain of 14 water molecules has been observed in the 2.6-Å crystal structure of the *Rhodobacter sphaeroides* reaction center extending from the **n**-side bulk aqueous phase through the peripheral protein mass associated with the "H" subunit to the proximal ether oxygen of the quinone (Ermler et al., 1994). This was proposed to be part of the pathway for proton uptake from the bulk phase into the membrane at the quinone Q_B site. A role of the water chain in the proton transfer pathway to Q_B was further implied by site-directed substitution (Pro L209 → Phe) at a position 9 Å from Q_B, which caused a sevenfold decrease in the rate constant for transfer of the second electron to Q_B (Baciou & Michel, 1995). Two high-p*K* carboxylate residues, Asp L213 and Glu L212, have also been implicated through site-directed substitution in the pathway of transfer of the first and second protons to Q_B (Paddock et al., 1989; Takahashi & Wraight, 1990, 1992; Rongey et al., 1993).

In bacteriorhodopsin, two widely separated carboxylates, Asp 85 and Asp 96, on opposite sides of helix C, are involved in proton transfer. A proton carrier system is needed to bridge the gap between these residues and the Schiff base, which is 10 Å from Asp 96. It has been estimated that at least 15 mol of bound water are required for maximal proton transfer to and from the retinal Schiff base (Cao et al., 1991). A difference density map obtained by neutron diffraction of purple membrane films at 15% relative humidity in D_2O showed approximately four water molecules close to the retinal (Papadopoulos et al., 1990).

The right-handed beta-helical dimer of the gramicidin A ion channel contains a linear chain of approximately 10 water molecules inside the channel (Roux et al., 1995). This chain may be somewhat disordered in the single-file transfer of ions other than H^+, but has been described as a "proton wire" when it acts as a highly conductive proton channel (Pomes & Roux, 1995).

Little is known about an intraprotein pathway of the coupled proton extrusion that accompanies oxidation of the cytochrome bc_1 or b_6f complex on the **p**-side of the membrane. The proton transfer occurs when ubiquinol is oxidized by the high potential electron acceptors of the complex, the Rieske iron-sulfur protein, and cytochrome c_1 or *f*. It has been reported recently that the major electrogenic event in the bacterial cytochrome bc_1 complex is proton and not electron transfer (Mulkidjanian & Junge, 1994). The proton transfer steps in *trans*-membrane proton translocation that do not involve the neutral quinol, and are therefore potentially electrogenic, are presumably in the interfacial or peripheral region of the membrane. This is the region occupied by the "H" subunit of the bacterial photosynthetic reaction center on the **n**-side of the membrane, and cytochrome c_1 or cytochrome *f* on the **p**-side.

Cytochrome *f* is the first subunit of the b_6f or bc_1 complexes for which the structure of a major active domain (a 252-residue C-terminal lumen-side fragment) has been solved to atomic (2.3 Å) resolution (Martinez et al., 1994). The present study concerns the extension of this structure to 1.96 Å, and its refinement. One of the major findings in the higher resolution refined structure is the presence of an extended, bound water chain whose unique properties suggest a possible function in a lumen-side exit port for proton translocation by the cytochrome b_6f complex (Kinemage 1).

Results

Comparison of structural results at 20° and −35°

The cooling of cytochrome *f* crystals was accompanied by a striking increase in diffraction intensity beyond 3 Å resolution. Figure 1A compares the diffracted intensity as a function of resolution for the 20° and −35° data sets. The sharper falloff of the 20° data is apparent. The −35° data are significantly stronger at high resolution, and have a lower R_{sym}. The lower average protein B for the −35° model compared to the 20° model is also apparent in Figure 1B.

Final statistics for the −35° and 20° structural models are given in Table 1. There are no residues in disallowed regions of the Ramachandran plots. A ribbon diagram of the cytochrome *f* molecule is shown in Figure 2. The largest conformational difference between the crystal structures of cytochrome *f* at 20° and at −35° is a rotation of one structural domain with respect to the other by 2.0°. Within the axial system of the crystals, the large domain rotated by 0.9° upon cooling, whereas the small domain rotated by 1.3°. The domain rotations are nearly addi-

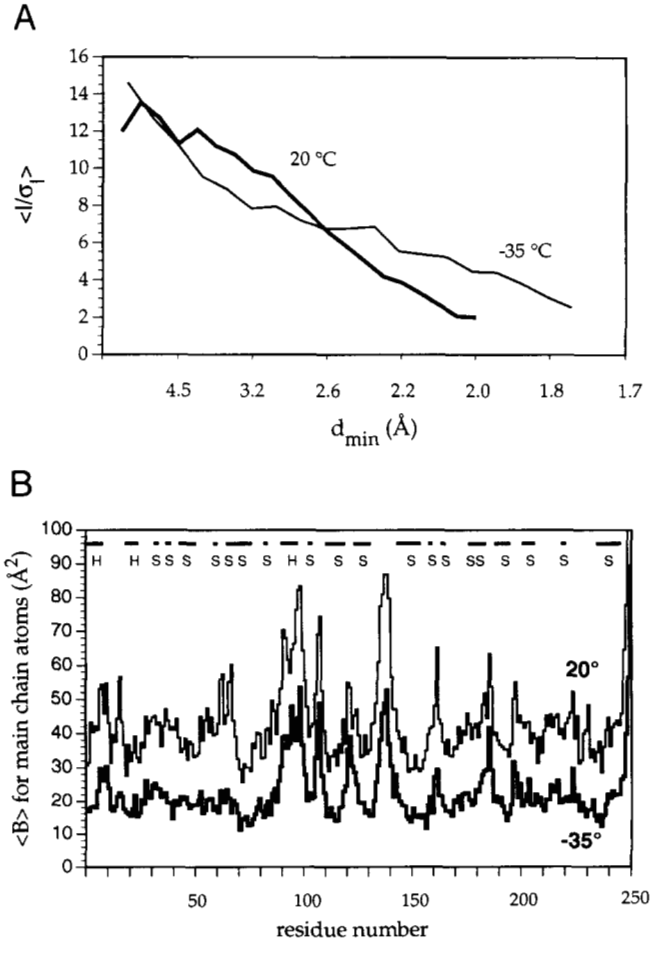

Fig. 1. A: Plot of average I/σ_I for the 20° and −35° diffraction data sets. **B:** Plots of average isotropic *B* factors for main-chain atoms in the 20° (top, thin line) and −35° (bottom, thick line) structural models of cytochrome *f*. The extents of secondary structure are indicated at the top. H, helix; S, beta strand.

Table 1. *Statistics on the refined structures of cytochrome* f *at 20° and −35°*

	20°	−35°
Range of data (Å)	∞–2.3	∞–1.96
Total # of reflections ($F > 1\ \sigma$)		
Working set (for R-factor)	11,723	19,639
Test set (for R-free)	599	986
No. non-H atoms	1,967	1,967
No. waters	413	408
R-factor[a]	14.0%	15.8%
R-free	29.3%	25.2%
Average isotropic B factor:		
Main chain (Å^2)	43.5	22.5
Side chain (includes heme) (Å^2)	51.3	30.7
Protein (includes heme) (Å^2)	46.9	26.5
Solvent (Å^2)	57.9	38.6
RMSDs from ideal geometry		
Bond lengths (Å)	0.013	0.013
Bond angles (°)	1.6	1.5
Torsion angles (°)	19.6	20.6
Estimated coordinate error (Å) (Luzzati, 1952)	0.23	0.20

[a] $R = \Sigma|F_o - F_c|/\Sigma|F_o|$.

tive, indicating that they were in nearly opposite directions. Other than the domain hinging, there are no substantial conformational differences between the 20° and −35° structures. The only substantial change to a single amino acid residue was a 120° rotation of the side chain of Gln 56, which occurs in a lattice contact. Gln 56 is on the back side of the large domain, and it contacts Gly 176, Asp 196, and Lys 222 at the top of the small domain in a neighboring molecule.

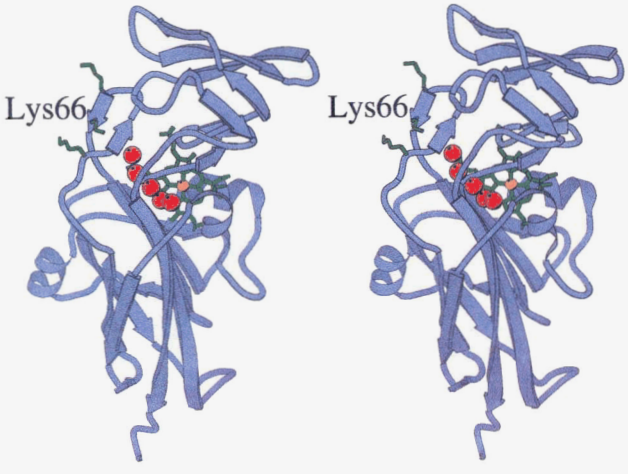

Fig. 2. Color stereo ribbon drawing of cytochrome *f*. Arg 250, the last residue showing order in the electron density map, which is connected to the trans-membrane anchor domain (not shown), is at the bottom center. The heme is shown in ball-and-stick representation with porphyrin ring in green and heme Fe in orange-brown. The buried five-water chain is in red. For clarity, the Tyr 1 and His 25 heme ligands are not shown. The position of Lys 66 is marked, with its side chain shown in green. The nearby side chains of Lys 58 and Lys 65 that contribute to a positively charged surface region are also in green.

There is a striking difference between the 20° and −35° structures of cytochrome *f* in the isotropic temperature factors (*B* values) for protein atoms. The final refined model from crystals at −35° had an average *B* for the protein of 26.5 Å^2, significantly less than the value of 46.9 Å^2 for the 20° model. Diffraction from 20° crystals was very strong at low resolution, but diminished rapidly such that average I/σ_I was less than 2.0 for data beyond 2.3-Å spacings. A less rapid falloff was observed in the data from crystals at −35°. A sharp transition between these two states was observed reproducibly near −28° during crystal cooling. Otherwise, equivalent diffraction images from the Siemens area detector had noticeably more diffraction spots at temperatures below the transition. A shrinkage of the *c*-axis by 2.4% occurred in conjunction with the transition in the diffraction pattern. The dramatic reduction in diffraction falloff and atomic *B* values is not simply explained upon examination of the lattice packing, but is doubtless due to the independent rotation of domains in the crystal lattice that accompanies cooling. Thus, the thermal transition is between related, but distinct, crystal forms.

The thermal transition of cytochrome *f* crystals is probably unrelated to the broad transition near −50° reported for the dynamic properties of crystalline ribonuclease A and other proteins (Rasmussen et al., 1992, and references therein), which was ascribed to anharmonic thermal motion of groups of atoms. In cytochrome *f* crystals, the transition near −28° was sharp and reproducible. Large temperature-dependent changes in *B* values were not a feature of ribonuclease A crystals. The thermal transition of cytochrome *f* crystals is correlated to the domain hinging and is therefore protein and lattice specific.

Structure of cytochrome f

The lumen-side segment of cytochrome *f* includes two structural domains (Fig. 2 and Kinemage 1). Main-chain hydrogen bonding diagrams are shown in Figure 3 for the two domains. The large domain consists of an antiparallel β sandwich and a short heme-binding peptide, which form a three-layer structure. This folding unit is a departure from other, predominantly helical, *c*-type cytochromes (Martinez et al., 1994). The small domain is inserted between β strands F and G of the large domain and is an all-β domain.

The β sandwich core of the large domain has the same fold as the well characterized fibronectin type III domain (FnIII). This β-sheet topology appears to have multiple, independent origins, because it has been observed in several unrelated proteins (Kim et al., 1993; Bork et al., 1994; Perrakis et al., 1994). Cytochrome *f* has no obvious sequence or functional relationship to any other protein with the FnIII fold.

The redox center heme nestles between two short helices at the amino terminus of cytochrome *f* (Kinemage 1). Within the second helix is the sequence fingerprint for the *c*-type cytochromes (Cys-X-Y-Cys-His, residues 21–25), which is covalently attached to the heme through thioether bonds to Cys 21 and Cys 24. His 25 is the fifth heme iron ligand. The sixth heme iron ligand is the α-amino group of Tyr 1 in the first helix.

The heme fits against the FnIII core β sandwich in a pocket that is well adapted to this role (Fig. 4). The A-B edge of the heme is parallel to β-strand βC and packed against this strand

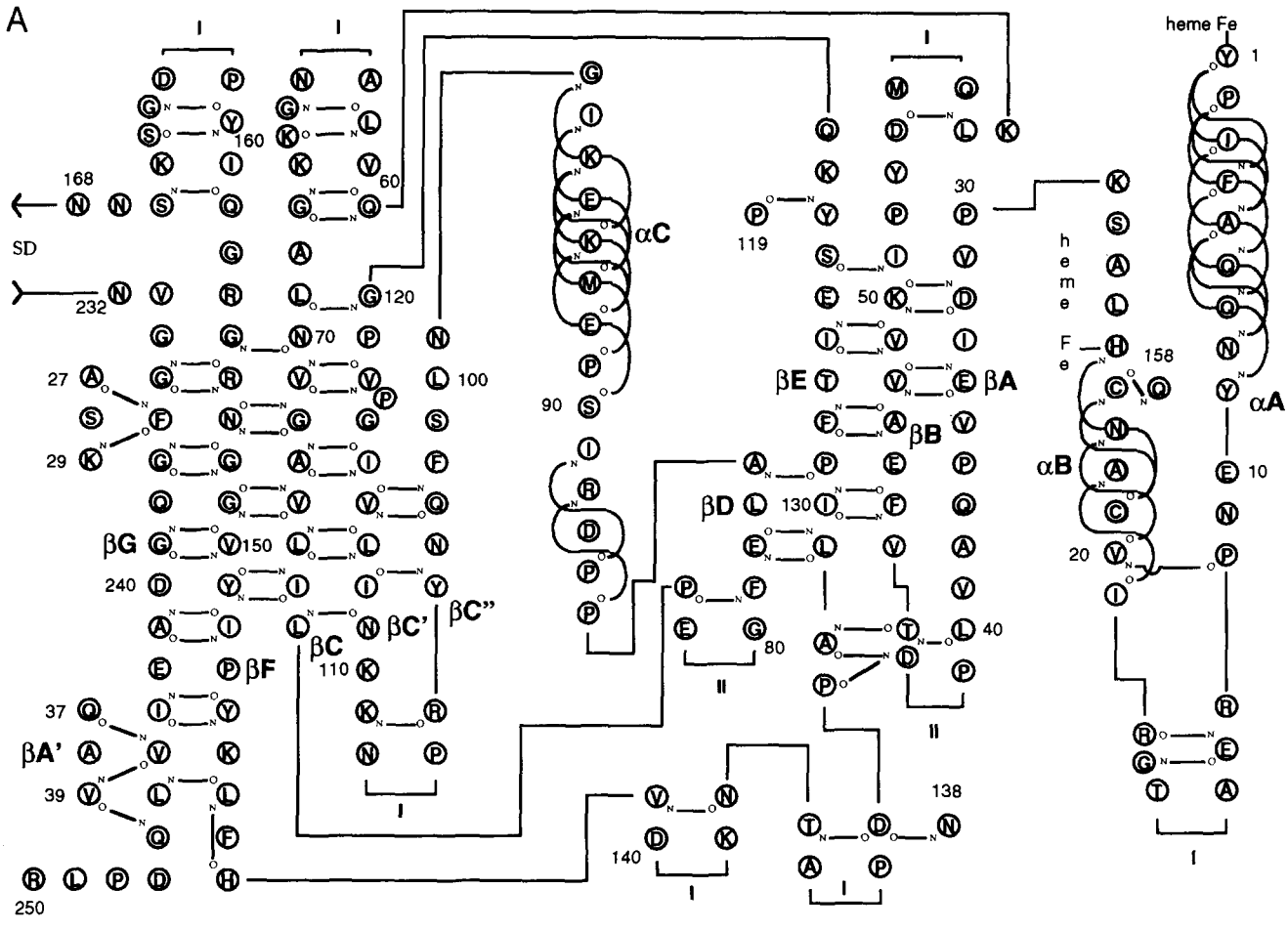

Fig. 3. Main-chain hydrogen bonding diagram for (**A**) the large domain (LD, residues 1-168, 232-250) and (**B**) the small domain (SD, residues 169-231) of cytochrome *f*. Reverse turns are denoted by type (Type I or II). (*Continues on facing page.*)

between residues 70 and 74. A glycine at position 72 ensures close packing of the heme against βC. Side chains from βF, βC, and βC′ form a pocket into which the A-B edge of the heme fits. The walls of the pocket are formed by Asn 70 and Val 74 in βC, by Val 114 and a wide β bulge at *cis* Pro 117 in βC′, and by Asn 153 and Gly 155 in βF. The A corner of the heme is bracketed by Asn 70, and the B corner by Val 74.

Water chain

Cytochrome *f* has an internal network of water molecules (Fig. 5 and Kinemage 1), which may be described as an L-shaped chain with one long (four waters) and one short (one water) branch. The longer branch extends 11 Å toward Lys 66, in the prominent basic patch at the top of the large domain. None of the waters is accessible to solvent at the surface of the protein. The waters are of high occupancy because their $F_o - F_c$ peaks were the highest or among the highest, and their *B* factors are comparable to those of polar protein atoms that they contact (Table 2). Density for these waters was present in the first electron density maps (Martinez et al., 1994). It is important to note that the shift from 20° to −35° does not affect the water cavity.

The water chain in cytochrome *f* possesses an array of hydrogen bonds in which donors and acceptors can be assigned definitively. Polar atoms within 3.5 Å of each water in the chain are listed in Table 2. For each water, 3-4 neighboring polar atoms have interatomic distances and angles favorable for hydrogen bonding to the water. The donor or acceptor status of each of the 12 protein atoms that are hydrogen bonded to the water chain can be established with certainty (Fig. 6 and Kinemage 1). Two hydrogen bonds are made to peptide nitrogen atoms and two to peptide oxygen atoms. The orientation of peptide planes is established by the electron density. Five hydrogen bonds are made to side-chain amide oxygens and two to amide nitrogens. In all these cases, the amide orientations, which are difficult to establish otherwise, are uniquely determined by other hydrogen bonds of the amides to peptide nitrogens or oxygens. The final hydrogen bond is to Nδ1 of His 25, which must be a proton donor at neutral pH because Nε2 of His 25 is a heme Fe ligand and is therefore unprotonated.

A neutral water molecule can donate its two protons in hydrogen bonds, whereas its two lone pairs of electrons can accept two protons in hydrogen bonds with donor atoms. Having established the donor/acceptor status of all protein atoms forming hydrogen bonds with the water chain, it may be possible to assign specific donor/acceptor roles in the water-water hydrogen bonds. This is the case for three hydrogen bonds within the water chain in cytochrome *f*, involving W1, W2, W3, and W4.

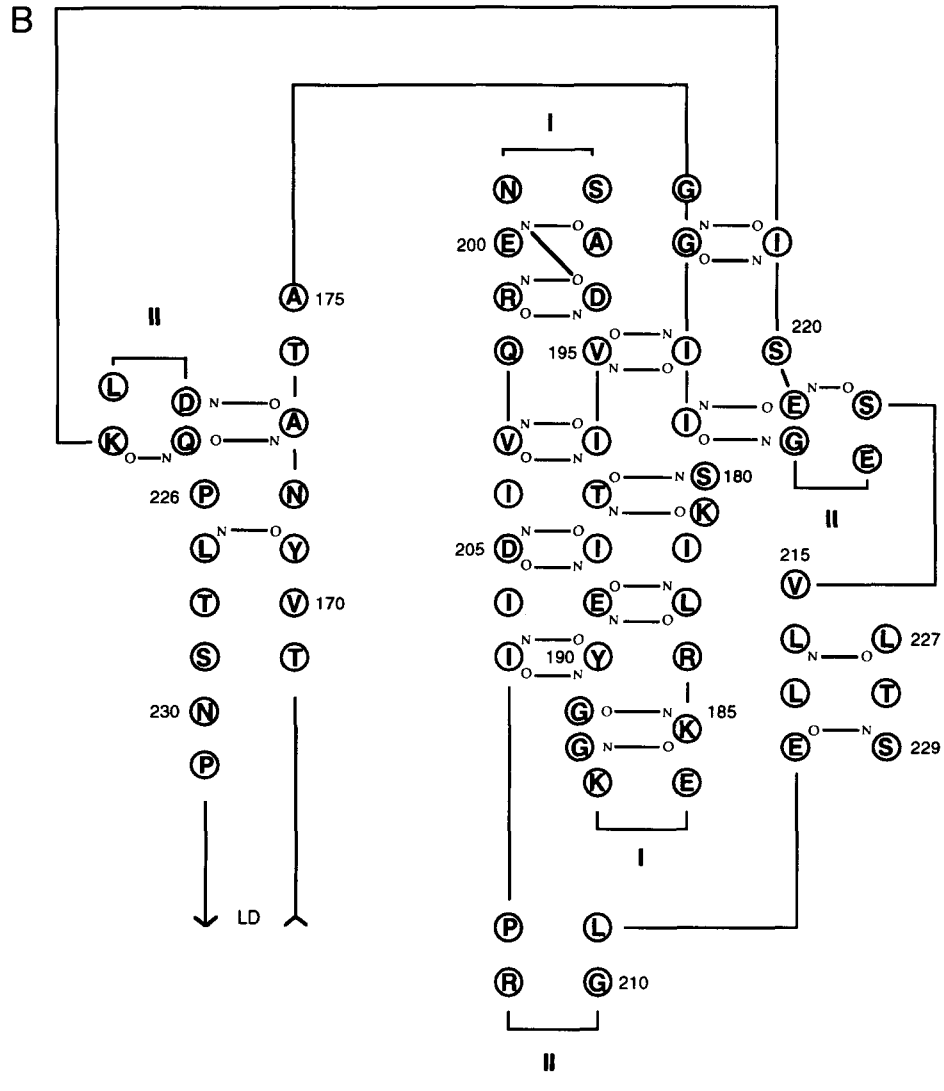

Fig. 3. *Continued.*

Between the final two waters in the chain, W4 and W5, there is a discrepancy of donor/acceptor status as both are predicted to be acceptors if all waters are neutral. Addition of a proton to W3, W4, or W5 would eliminate the discrepancy. Alternatively, a hydrogen bond may not exist between W4 and W5 because of their rather long (3.5 Å) separation (Table 2).

The water chain appears to be a conserved feature of cytochrome *f*. Virtually all residues forming hydrogen bonds with the water chain, whether through their main-chain or side-chain atoms, are invariant among 13 cytochrome *f* sequences (Gray, 1992). The lone exception occurs in the sequence from the bean *Vicia faba*, where Thr (codon ACC) was reported at position 153 (Ko & Straus, 1987) instead of Asn (possible codon, AAC) as in all other cytochrome *f* sequences.

pH Dependence of cytochrome f *oxidation-reduction potential*

The oxidation state of turnip cytochrome *f*, as well as its electron acceptor plastocyanin, was titrated as a function of redox potential and pH. The midpoint potential, E_m, of cytochrome *f* is shown as a function of pH (Fig. 7). The cyt *f* E_m is approximately constant, +370 mV, in the pH interval 4.5–8.0 (cf. Davenport & Hill, 1952; Rich & Bendall, 1980). At pH 5.0, close to that in the thylakoid lumen, the E_m of plastocyanin was +400 mV (data not shown). The E_m of cyt *f* decreases monotonically at alkaline pH, with a $pK \approx 8.5$.

Discussion

Buried water chains

Large, buried water clusters are a rare structural feature of proteins. In a survey of 75 nonhomologous high-resolution (2.5 Å) protein structures, fewer than seven buried water clusters with five or more waters were identified (Williams et al., 1994). In this survey, most waters, single or clustered, were buried below one layer of protein atoms. Four of the five cytochrome *f* waters are buried to this extent, whereas W2, which is hydrogen bonded to His 25 Nδ1, is more deeply buried. The cyt *f* W2–W5

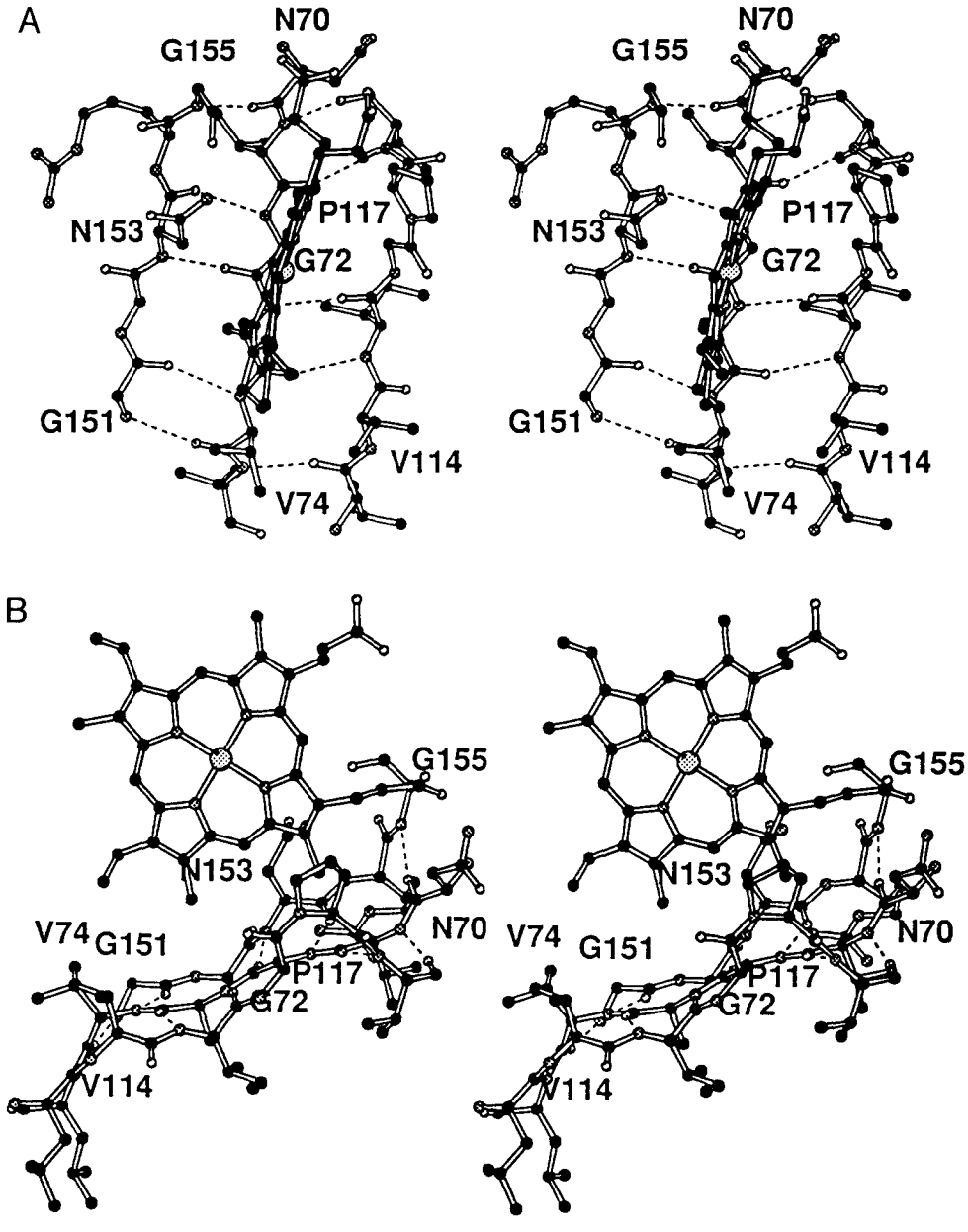

Fig. 4. Perpendicular stereo views of the packing of the heme group against the core of the large domain. **A:** Edge-on view of the heme. **B:** Front view of the heme. Parts of β-sheet C, C′, and F (see text), utilizing the labeled residues, form a pocket for the A-B heme edge.

water chain, extending over approximately 11 Å, is the longest linear or quasi-linear chain except for the 14 H_2O chain extending over 23 Å in the photosynthetic reaction center (Ermler et al., 1994). As discussed above, the water chain in cytochrome *f* also appears to be conserved. Both its rarity and conservation support the argument that the water chain has a specific function in cytochrome *f*.

Cytochrome f *water chain as a proton wire*

The existence, in an energy-transducing membrane, of an internal water chain within a protein complex that also translocates protons naturally leads to the hypothesis that the water chain functions as a proton wire (Nagle & Morowitz, 1978). We propose that the internal water chain of cytochrome *f* is such a proton wire. Cytochrome b_6f can translocate 1–2 protons into the chloroplast lumen for each electron it transfers from plastoquinol to plastocyanin (data summarized in Cramer et al., 1987). The protons are derived from plastoquinol, and proton translocation is coupled to electron transfer. The role of protein components of the cytochrome b_6f complex in the pathway for proton transfer from the quinol to the lumen has not been considered previously.

Several features of the cytochrome *f* water chain make it an ideal redox-linked proton wire. The proximity of the water chain to the redox-active heme group provides a means of coupling

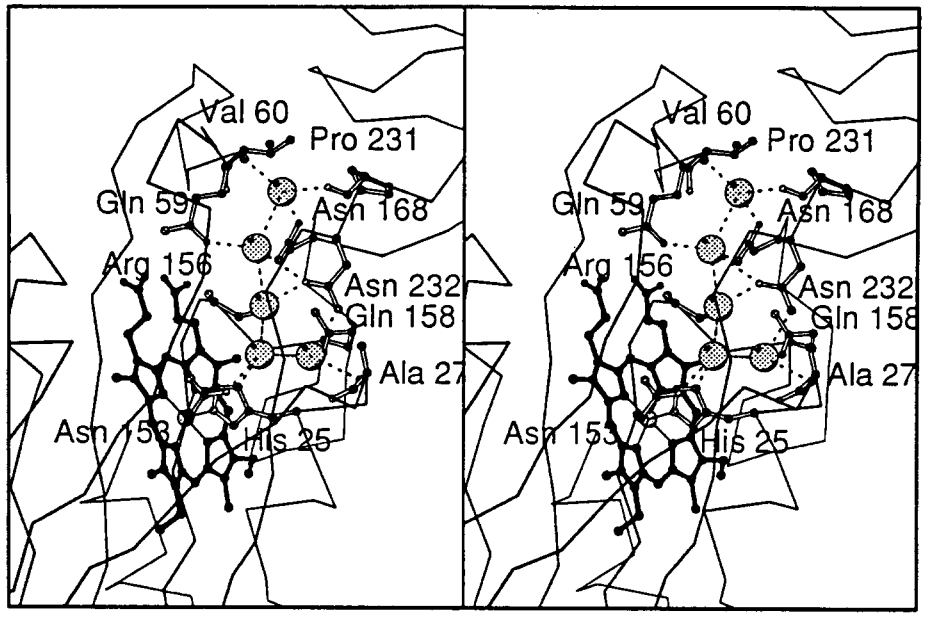

Fig. 5. The buried five-water chain within the context of the cytochrome *f* structure. The protein backbone is shown as a Cα trace. Waters are represented by spheres of less than Van der Waals radii. Hydrogen bonds to nearby polar atoms are also shown. Following the water chain from bottom to top, water identifiers are: W1, W2, W3, W4, and W5.

electron transfer to proton translocation. This coupling is suggested by aspects of the structure, e.g., the suggested proton wire function of the water chain and the fact that the chain is directed at Lys 66, suggested to be part of the docking site for plastocyanin (Martinez et al., 1994). However, because little is known at present about the mechanisms of long-range H^+ translocation through proteins, or about mechanisms for coupling electron and H^+ transfer, the coupling mechanism proposed here

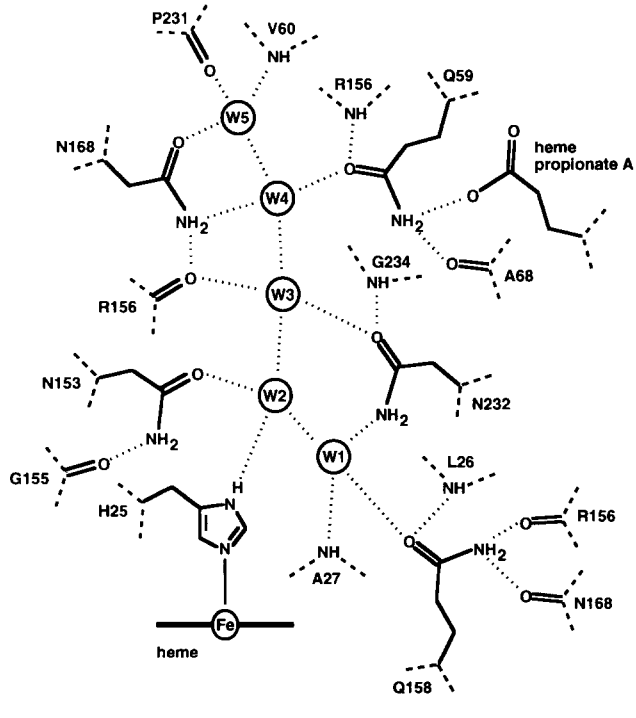

Fig. 6. Schematic diagram of the hydrogen bonding environment of the buried water chain of cytochrome *f*. Hydrogen bonds are drawn in dotted lines; covalent connections to the protein backbone are in dashed lines; covalent bonds in side chains and in main-chain carbonyl groups are in solid lines.

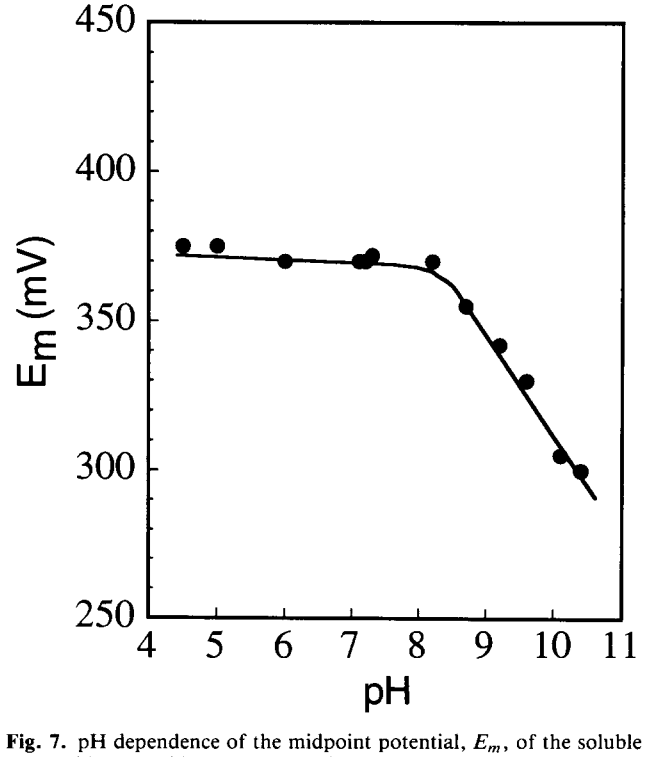

Fig. 7. pH dependence of the midpoint potential, E_m, of the soluble lumen-side 252 residue cytochrome *f* fragment from turnip chloroplasts (Gray, 1992; Martinez et al., 1994). Reduced minus oxidized spectra were measured for cytochrome *f* as a function of the ambient redox potential, as described in the Materials and methods.

Table 2. *Polar atoms within 3.5 Å of the cytochrome f five-water chain*

Water atom			Neighbor atom			
Identifier[a]	Occupancy	*B* (Å^2)	Polar contact	*B* (Å^2)	H-bonding role[b]	Distance (Å)
W1	0.9	10.8	W2	14.4	A	2.7
			N232 Nδ2	15.1	D	2.9
			A27 N	17.2	D	3.1
			Q158 Oε1	19.7	A	2.8
			L26 N	20.0		3.3
W2	1.0	14.4	W1	10.8	D	2.7
			W3	12.0	A	2.7
			H25 Nδ1	11.2	D	3.1
			N153 Oδ1	12.9	A	2.8
			R154 O	19.1		3.2
			G235 N	9.3		3.3
			G155 O	14.6		3.3
W3	1.0	12.0	R156 O	15.6	A	2.8
			W2	14.4	D	2.7
			W4	15.9	D	3.1
			N232 Oδ1	15.5	A	2.5
			G234 N	14.1		3.5
W4	0.9	15.9	W3	12.0	A	3.1
			N168 Nδ2	16.8	D	3.0
			Q59 Oε1	17.1	A	2.9
			W5	14.8		3.5
			V233 N	16.0		3.4
			G234 N	14.1		3.3
			N232 Oδ1	15.5		3.2
W5	1.0	14.8	V60 N	15.4	D	2.9
			W4	15.9		3.5
			N168 Oδ1	16.3	A	2.7
			P231 O	20.7	A	2.6

[a] Waters are named sequentially for clarity. In the Protein Data Bank (PDB) entry, correspondences are as follows: W1, PDB W15; W2, PDB W1; W3, PDB W4; W4, PDB W21; W5, PDB W3.

[b] The donor (D) or acceptor (A) status of each neighbor atom with favorable interatomic angles for hydrogen bonding to the waters is indicated.

cannot be considered obligatory. However, addition of a proton to the water chain at the same time an electron is transferred to the heme would result in no change to the net charge of the heme environment. The same charge balance would be maintained by release of a proton from the water chain simultaneously with oxidation of cytochrome *f* by plastocyanin. As described above, the donor/acceptor balance of the water chain in reduced cytochrome *f* lacks one donor if each water is neutral. Storage of a proton on W3, W4, or W5 would balance the donors and acceptors in the water chain.

The water chain/proton wire is "insulated" from the surrounding protein. None of the protein hydrogen bonding partners to the water chain is capable of being both a proton donor and an acceptor at normal pHs, and none is an ionizable group under normal conditions. Thus, the alternating scheme of hydrogen bond donors and acceptors, as expected for a proton wire, can only function along the water chain itself. Protons cannot escape to, nor be derived from, the protein medium.

Coupling of proton translocation to electron transfer through cytochrome *f* may be facilitated by the closed ends of the water chain. In the uncomplexed, reduced form of cytochrome *f* seen in the crystal structure, none of the five waters in the chain is accessible to bulk solvent. Movement of at least protein side chains is needed to open the water chain to the external environment. Access to the water chain for uptake or release of a proton could occur when cytochrome *f* forms productive complexes with its redox partners, the electron acceptor, plastocyanin, and donor, the Rieske [2Fe-2S] protein.

A relationship between the water chain and plastocyanin association with cytochrome *f* seems likely. The uppermost water molecule, W5, in Figures 2, 5, and 6, is at the interface between the large and small domains of cytochrome *f*, very near to the positive surface patch that has been suggested to participate in the docking of plastocyanin (Martinez et al., 1994). The side chains of Lys 58, Lys 65, and Lys 66 of this patch are within 10 Å of W5. Thus, plastocyanin binding to cytochrome *f* is a candidate for triggering small structural changes to open the water chain at W5. The plastocyanin midpoint potential (E_m = +400 mV at pH 5, +370 mV at pH 7, data not shown) makes it approximately isopotential for electron transfer with cytochrome *f*. Two groups of carboxylate residues in plastocyanin, Asp 42–44 and Glu 59, 60 (Gross, 1993) are candidates for docking to cytochrome *f*. One or more of these carboxylates could act as a proton sink for proton transfer from the water chain. Protonation and neutralization of a plastocyanin carboxylate linked to the electron transfer would also provide a mechanism for release of reduced plastocyanin from cytochrome *f*.

There are no data bearing directly on the association of cytochrome *f* with its electron donor. Because of its weak optical signal, the electron transfer properties of the Rieske protein in situ have been less well studied than those of cytochrome *f*. If W5 of the water chain connects cytochrome *f* and plastocyanin, then it is inferred that W1 forms the proton connection with the Rieske protein. W1 is hydrogen bonded to Asn 232 and Gln 158, and is within 3.5 Å of His 25, Leu 26, and Ala 27, the latter a residue exposed at the protein surface.

Mechanism of proton transfer in the water chain

If the water chain in cytochrome *f* participates in proton translocation, then the driving force for proton uptake or release would be a change in the electrostatic field of cytochrome *f* upon electron transfer. The proximity of the water chain to the heme in cytochrome *f* provides a means for linking the protonation state of the water chain to the oxidation state of the protein. The mechanism for proton transfer must provide one or more residues from the complex that could inject a proton into the cytochrome *f* water chain. The identity of this residue(s) is unknown, but is limited by established features of the complex. Quinol is the ultimate electron and proton donor to cytochrome b_6f. The binding site of the quinol is near the [2Fe-2S] center of the Rieske protein and probably involves the peripheral "cd" and "ef" helices of cytochrome b_6 (Cramer et al., 1994a). Association of the Rieske protein, cytochrome *f*, and the cytochrome b_6 surface helices is expected to induce redox-linked p*K* shifts in one or more residues that are at the protein–protein interface and

near the water chain of cytochrome *f*. Appropriate p*K* shifts would decrease the p*K*s of protonated acidic or basic groups upon reduction of cytochrome *f* by the Rieske protein, such that a proton would be released into the water chain. Stated another way, proton movement responds to a change in the electrostatic field when an electron is transferred from the Rieske [2Fe-2S] center to the cytochrome *f* heme. If the water chain functions in proton translocation, then proton uptake must be from a component of the cytochrome b_6f complex. However, proton release in response to oxidation of cytochrome *f* could be directly to the lumen or via the electron acceptor plastocyanin.

If a proton is "stored" in the water chain of reduced cytochrome *f*, then the hydrogen bonding donor/acceptor balance and the local electrostatic field of the protein dictate which water(s) the proton occupies. By donor/acceptor accounting, a proton could be stored on W3, W4, or W5 without rearrangement of the protein structure. On the other hand, small structural rearrangements of the protein are necessary to insert or remove a proton. These are not large, and the water chain is expected to exchange with bulk solvent during normal dynamic fluctuations of the protein. The proton balance within the water chain is maintained by the local electrostatic field of the protein, to which the oxidation state of the heme is a major contributor. Further, the water chain is the most likely site of charge balance for the heme due to its isolation from bulk solvent and the absence of other titratable groups in the heme environment. Structural changes to cytochrome *f* that occur upon binding to redox partners are expected to facilitate proton transfer by displacing hydrogen bonding groups from the ends of the water chain. A cytochrome *f* hydrogen bonding group could be replaced by the appropriate proton donor in the Rieske protein or proton acceptor in plastocyanin, for example.

pH dependence of cytochrome f *midpoint potential*

The absence of a pH-dependent E_m in the pH range 4.5–8.0 (Fig. 7) might argue that H^+ transfer is not coupled to electron transfer in cyt *f*. However, these titrations were performed under equilibrium conditions. Under such conditions, the pH dependence of the E_ms of the proton pumping cytochrome oxidase are also not striking (Wikström et al., 1981). One might expect that the effect of proton transfer function on the E_m associated with electron transfer is readily observable only under the non-equilibrium conditions of the functioning membrane, as demonstrated in the pH-dependent E_m values associated with H^+ uptake to the Q_B site in the photosynthetic reaction center (Paddock et al., 1989, 1994; Takahashi & Wraight, 1990, 1992).

The observation of a p*K* at approximately 8.5 in the redox function of cytochrome *f* (Fig. 7) might be considered a significant clue to further insight into its proton transfer function. The chemical group(s) responsible for the observed p*K* of 8.5 is (are) expected to be near the heme. The heme sits in a largely hydrophobic pocket where there are few amino acids with titratable side chains. The list of possible residues includes Tyr 1, Tyr 160, His 25, and the heme propionate groups. Neither the Tyr 1 amino group nor the His 25 Nϵ2 are possibilities, because they are Fe ligands. In mitochondrial cytochrome *c*, a transition with p*K* greater than 9 has been attributed to one of the two buried heme propionates (Hartshorn & Moore, 1989; Moore & Pettigrew, 1990). This is unlikely in cytochrome *f* because neither propionate is buried in a hydrophobic environment. The hydrogen bonding network involving the propionates indicates that they are deprotonated under all relevant conditions. The D propionate tail (on the D pyrrole ring) makes a double salt bridge to the guanidinium of Arg 156. Both of the A and D propionate tails are also solvent accessible, and their p*K*s are not expected to be perturbed from normal values (4–5). Similarly, the hydroxyl groups of Tyr 1 and Tyr 160 are solvent-exposed and also not expected to have abnormal p*K* values. The transition most likely responsible for the p*K* near 8.5 is deprotonation of His 25 Nδ1. Although the p*K* for the second proton of imidazole is 14.4 in water (Yagil, 1967), it appears to be lowered in histidine transition metal complexes because the negative charge formed upon deprotonation can be partially delocalized to the positively charged metal, as suggested by an Nδ1 p*K* of 8.8 in pentamineruthenium histidine (Sundberg & Gupta, 1973). p*K* values ranging from 9.0 to 10.4 in *Chironomus* methemoglobin and sperm whale myoglobin have been interpreted in terms of acidification of Nδ1 (Mohr et al., 1967; Morishima et al., 1980). In summary, it seems unlikely that the His 25 Nδ1 p*K* 8.5 group has a role in a physiological proton translocation mechanism. Unlike the environments of the Q_B site in the bacterial reaction center and the critical Asp residues in bacteriorhodopsin, the environment of cytochrome *f* in the thylakoid lumen is acidic. The lumen pH is 4.5–6.0 for a stromal pH of 8, the range of values reflecting the phosphorylation state of the membranes and the probe used to measure the *trans*-membrane ΔpH (Rottenberg & Grunwald, 1973). Thus, a group with a p*K* of 8.5 in the oxidized form, and an even more alkaline p*K* when reduced, could not be deprotonated unless it is completely shielded from the external pH. In fact, an unprotonated His 25 Nδ1 nitrogen with p*K* 8.5 might act as a dead-end bypass for H^+ transfer in the water chain.

If cytochrome *f* functions in proton transfer, then the available data suggest that its proton donor is the Rieske protein, which is the proton and electron acceptor of plastoquinol. A proton transfer function was proposed for the Rieske protein of the mitochondrial cytochrome bc_1 complex, based on p*K* values of the midpoint potential at 7.6 and 9.2, measured by cyclic voltammetry in a soluble C-terminal fragment (Link et al., 1992, 1993). However, if the protein interior senses the ambient pH, such a Bohr effect seems implausible for the Rieske protein of cytochrome b_6f because of the acidic environment of the chloroplast lumen. [In titrations of the midpoint potential of a C-terminal fragment of the chloroplast Rieske protein, no pK has been found between pH 6 and 7 (H. Zhang, D. Huang, V. Sled, T. Ohnishi, & W.A. Cramer, unpubl. data)].

Other roles for the water chain of cytochrome f

Functions for the water chain in cytochrome *f* other than participation in proton translocation should be considered. The water chain may participate in signaling the oxidation state of the heme. Small redox-linked changes in the heme-His 25 pair may induce changes in the water chain that are accompanied by changes in groups on the surface of the protein. This would effectively signal to redox partners the oxidation state of cytochrome *f*.

Precedent for such an effect is found in NMR studies of cytochrome *c*. Structural water has been detected in the interior of oxidized and reduced horse-heart cytochrome *c* (Qi et al., 1994b). Of the two waters whose NOE distances locate them near the heme crevice, the position of one is dependent on oxi-

dation state, implying that it could affect the solvent reorganization energy associated with electron transfer. Movement of the surface residue Ile 81 is also associated with the oxidation state of cytochrome *c* and has been proposed as a redox signal (Qi et al., 1994a).

Materials and methods

Purification and crystallization

The 252-residue lumen-side domain of cytochrome *f* was purified from turnip (*Brassica campestris*) leaf chloroplasts and crystallized at 5–9 °C by a capillary vapor diffusion method as described previously (Martinez et al., 1992). The crystals belong to the orthorhombic space group $P2_12_12_1$ and have one 27.5-kD lumen-side domain per asymmetric unit. The crystals of reduced cytochrome *f* are orange-red bipyramids that grew to a maximum length of 0.5 mm on a side. At room temperature (20°), diffraction to 2.0-Å resolution has been observed. The transform has a sharp decrease in intensity beyond 3.0 Å.

Data collection

A native room-temperature data set was collected as previously reported (Martinez et al., 1994). A low temperature data set was collected from five crystals at $-35 \pm 2°$. Before cooling, crystals were mounted in glass capillary tubes in equilibrium with a plug of mother liquor (50% acetone, 40 mM MES, 1 mM DTE, pH 6.5). Both ends of the capillary were filled with plugs of mineral oil and one end was sealed with wax. The mineral oil plug in the open end of the capillary served as a mobile seal, allowing the trapped capillary air volume to decrease as the temperature was reduced. After orienting the capillary parallel to the vertical airflow, the temperature was lowered from room temperature to 10°, and then decreased in 10° decrements. Individual steps were usually of 10-min duration, and occasionally 15–30 min. Cooling was monitored with a thermocouple element, placed in the air stream as close to the crystal as possible, but not in contact with the capillary tube. Most of the data were collected using a dry nitrogen gas enclosure, which surrounded the entire camera. Data from five crystals were collected using CuKα radiation and a Xentronics 100/Siemens area detector. Data statistics are summarized in Table 3.

Refinement

The 2.3-Å structure of cytochrome *f* at room temperature (20°) was reported previously (Martinez et al., 1994). Subsequent refinement of this model was conducted in order to identify additional ordered solvent and to investigate the unusually large protein *B* factors. Three-hundred additional solvent molecules were added in five rounds of refinement using the program TNT. The average *B* factor of 47 Å^2 for protein atoms seemed high for crystals that diffract to 2.0 Å. It was possible to reduce the average refined *B* to 31 Å^2 by fixing the overall scale factor for F_{calc} to an appropriate value. However, this approach was not pursued because it had the anticipated effect of systematic overestimation of F_{calc} at high resolution and underestimation at low resolution. Inclusion of data within the 6-Å sphere resulted in slightly lower values for protein B and improved the protein density in a few parts of the model.

Table 3. *Summary of statistics for the 20° and −35° data sets*

Data set	20°	−35°
a (Å)	79.2	78.6
b (Å)	81.9	82.2
c (Å)	46.3	45.2
No. crystals	4	5
d_{min} (Å)	2.3	1.96
R_{sym}[a] (%)	5.1	6.8
No. observations	52,944	86,869
No. reflections	13,189	21,059
Completeness (%)	94.7	97.2
Redundancy	4.0	4.1
Average I/σ_I	7.9	6.9

[a] $R_{sym} = \Sigma_{hj} \left| I_h - I_j \right| / \Sigma_j I_j$, where I_h = average intensity over symmetry-related observations of a reflection with unique indices and $I_j = j$th observation of a reflection with average intensity I_h.

Resolution-dependent weights (w) were applied to individual F_{obs} for the 20° data set, where $w = 1/(A + B(\sin\theta/\lambda - C))^2$, with $A = 1$, $B = -5.0$, and $C = 0.172$. This weighting scheme was implemented in TNT by replacing individual reflection σ_F values with $(A + B(\sin\theta/\lambda - C))$ outside of TNT and selecting the $1/\sigma^2$ weighting option inside the program. The user-selected overall reflection weight, which balances stereochemical and F_{obs} contributions to the minimization, is applied after these weights. Parameter selection of $A = 1.0$ and $C = \sin\theta/\lambda$ near the mid-range of the data set ensured that the total weight applied to structure factors did not vary significantly from the user-selected weight and that the X-ray terms remained in balance with stereochemical terms. The slope of the weighting curve is determined by the parameter *B*, which was selected here to down-weight low-resolution data such that average $w(F_{obs} - F_{calc})^2$ was approximately flat across the resolution range. The resolution-dependent weighting scheme had virtually no effect on the *B* factors of the protein model. Unit weights were used for the −35° data set.

Cooling of cytochrome *f* crystals to −35° was accompanied by changes in cell constants of up to 2.4% (Table 3). The final 20° model was rigid-body refined against 8.0–2.5-Å data of the −35° data set. The *R*-factor dropped from 46.7% to 36.0%. The small domain (169–231) and the large domain (residues 1–168, 232–250, and the heme) of the cytochrome were then refined as separate rigid bodies, reducing the *R*-factor to 35.0%. Altogether, 10 rounds of refinement and manual adjustment of the model were done.

Solvent molecules in both models were added at positions of approximately spherical $2F_o - F_c$ density or $F_o - F_c$ density that were within hydrogen bonding distances (<3.5 Å) of a polar protein atom or another water. *B* factors were refined for waters; occupancies were not. The occupancies were set according to the height of their $F_o - F_c$ difference peaks. The strongest peaks in the initial $F_o - F_c$ maps were assumed to represent fully occupied water sites. Candidate water peaks, after inspection for hydrogen bonding geometry, were assigned occupancies on a linear scale, such that no fractional occupancy was less than 0.3. Waters that refined to distances greater than 3.6 Å from any potential hydrogen bonding partner or had *B* values among the top

5% of all waters were removed from the models. A total of 413 and 408 waters were included in the final 20° and −35° models, respectively. Refinement was complete when the strongest $F_o - F_c$ density could not be interpreted as errors in the protein model or as additional ordered solvent. Statistics for the final 20° and −35° models are given in Table 1. No multiple conformers were included in either protein model. The 20° and −35° models have been deposited in the Brookhaven Protein Data Bank.

Determination of the pH dependence of the cytochrome f *midpoint potential*

Turnip cytochrome *f* (dialyzed to remove dithionite in storage buffer) was titrated at a concentration of 0.5–0.75 μM (based on $\Delta\epsilon = 20\ mM^{-1}\ cm^{-1}$) in 50 mM buffer (dimethyl glutaric acid, MES, MOPS, HEPES, Tris, CAPS, depending on pH), 30 mM NaCl, and 5 mM EDTA. The initial potential was set by addition of 2 mM potassium ferricyanide from a 1 M freshly prepared stock solution. Titrations of the potential were carried out by adding aliquots of ascorbate from stock solutions of 0.2 M or 0.02 M for which each addition decreased the potential by approximately 20 mV. The potential was detected with a home-built platinum electrode system using Ag-AgCl (E_{ref} = +200 mV) as the reference electrode and ferri-ferrocyanide to vary the ambient redox potential. The electrode was calibrated using saturated quinhydrone and a standard potential of +699 mV (Clark, 1960).

Acknowledgments

We thank J. Hollister for her dedicated and skillful assistance with this manuscript, and J. Krahn for helpful discussions. These studies were supported by grants from the USDA (9301586) and NIH (GM-38323).

References

Baciou L, Michel H. 1995. Interruption of the water chain in the reaction center from *Rhodobacter sphaeroides* reduces the rates of the proton uptake and the second electron transfer to Q_B. *Biochemistry 34*:7967–7972.

Bork P, Holm L, Sander C. 1994. The immunoglobulin fold: Structural classification, sequence patterns and common core. *J Mol Biol 242*:309–320.

Cao Y, Varo G, Chang M, Ni B, Needleman R, Lanyi JK. 1991. Water is required for proton transfer from aspartate 96 to bacteriorhodopsin Schiff base. *Biochemistry 30*:10972–10979.

Clark WM. 1960. *Oxidation-reduction potentials of organic systems*. Baltimore: Williams and Wilkins. p 375.

Cramer WA, Black MT, Widger WR, Girvin ME. 1987. Comparative structure and function of the *b* cytochromes of *b*-c_1 and b_6-*f* complexes. In: Barber J, ed. *The light reactions*. Amsterdam: Elsevier Sci. Publ. pp 446–493.

Cramer WA, Martinez SE, Furbacher P, Huang D, Smith JL. 1994a. The cytochrome b_6f complex. *Curr Opin Struct Biol 4*:536–544.

Cramer WA, Martinez SE, Huang D, Tae GS, Everly RM, Heymann JB, Cheng RH, Baker TS, Smith JL. 1994b. Structural aspects of the cytochrome b_6f complex; structure of the lumen-side domain of cytochrome I. *J Bioenerg Biomem 26*:31–47.

Davenport HE, Hill R. 1952. The preparation and some properties of cytochrome *f*. *Proc R Soc London B 139*:327–345.

Ermler U, Fritzsch G, Buchanan S, Michel H. 1994. Structure of the photosynthetic reaction centre from *Rhodobacter sphaeroides* at 2.65 Å resolution: Cofactors and protein-cofactor interactions. *Structure 2*:925–936.

Gray J. 1992. Cytochrome *f*: Structure, function, and biosynthesis. *Photosyn Res 34*:359–374.

Gross EL. 1993. Plastocyanin: Structure and function. *Photosyn Res 37*:103–116.

Hartshorn T, Moore GR. 1989. A denaturation-induced proton-uptake study of horse ferricytochrome *c*. *Biochem J 258*:595–598.

Henderson R, Baldwin JM, Ceska TA, Zemlin F, Beckmann E, Downing KH. 1990. Model for the structure of bacteriorhodopsin based on high-resolution electron cryo-microscopy. *J Mol Biol 213*:899–929.

Kim KH, Kwon BM, Myers AG, Rees DC. 1993. Crystal structure of neocarzinostatin, an antitumor protein-chromophore complex. *Science 262*:1042–1046.

Ko K, Straus NA. 1987. Sequence of the apocytochrome *f* gene encoded by the *Vicia faba* chloroplast genome. *Nucleic Acids Res 15*:2391.

Lanyi JK. 1993. Proton translocation mechanism and energetics in the light-driven pump bacteriorhodopsin. *Biochim Biophys Acta 1183*:241–261.

Link TA, Haase U, Brandt U, von Jagow G. 1993. What information do inhibitors provide about the structure of the hydroquinone oxidation site of ubihydroquinone: Cytochrome *c* oxidoreductase? *J Bioenerg Biomem 25*:221–232.

Link TA, Hagen WR, Pierik AJ, Assmann C, von Jagow G. 1992. Determination of the redox properties of the Rieske [2Fe-2S] cluster of bovine heart bc_1 complex by direct electrochemistry of a water-soluble fragment. *Eur J Biochem 208*:685–691.

Luzzati PV. 1952. Traitement statistique des erreurs dans la determination des structures cristallines. *Acta Crystallogr 5*:802–810.

Malkin R. 1982. Interaction of photosynthetic electron transport inhibitors and the Rieske iron-sulfur center in chloroplasts and the cytochrome b_6f complex. *Biochemistry 21*:2945–2950.

Martinez SE, Huang D, Szczepaniak A, Cramer WA, Smith JL. 1994. Crystal structure of chloroplast cytochrome *f* reveals a novel cytochrome fold and unexpected heme ligation. *Structure 2*:95–105.

Martinez SE, Smith JL, Huang D, Szczepaniak A, Cramer WA. 1992. Crystallographic studies of the lumen-side domain of turnip cytochrome *f*. In: Murata N, ed. *Research in photosynthesis, vol II*. Dordrecht: Kluwer. pp 495–498.

Mohr P, Scheler W, Schumann H, Müller K. 1967. Ligand-protein interactions in imidazole and 1,2,4-triazole complexes of methaemoglobin from *Chironomus plumosus*. *Eur J Biochem 3*:158–163.

Moore GR, Pettigrew GW. 1990. *Cytochromes c: Evolutionary, structural, and physicochemical aspects*. Berlin: Springer-Verlag. pp 344–361.

Morishima I, Neya S, Yonezawa T. 1980. Proton NMR study of hemoproteins: Ionization and orientation of iron-bound imidazole in methemoglobin and metmyoglobin. *Biochim Biophys Acta 621*:218–226.

Mulkidjanian AY, Junge W. 1994. Calibration and time resolution of lumenal pH-transients in chromatophores of *Rhodobacter capsulatus* following a single turnover flash of light: Proton release by the cytochrome bc_1-complex is strongly electrogenic. *FEBS Lett 353*:189–193.

Nagle J, Morowitz H. 1978. Molecular mechanisms for proton transport in membranes. *Proc Natl Acad Sci USA 75*:298–302.

Paddock ML, Rongey SH, Feher G, Okamura MY. 1989. Pathway of proton transfer in bacterial reaction centers: Role of aspartate-L213 in proton transfers associated with reduction of quinone to dihydroquinone. *Proc Natl Acad Sci USA 86*:6602–6606.

Paddock ML, Rongey SH, McPherson PH, Juth A, Feher G, Okamura MY. 1994. Pathway of proton transfer in bacterial reaction centers: Replacement of glutamic acid 212 in the L subunit by glutamine inhibits quinone (secondary acceptor) turnover. *Biochemistry 33*:734–745.

Papadopoulos G, Dencher NA, Zaccai G, Bueldt G. 1990. Water molecules and exchangeable hydrogen ions at the active centre of bacteriorhodopsin localized by neutron diffraction. *J Mol Biol 214*:15–19.

Perrakis A, Tews I, Dauter Z, Oppenheim AB, Chet I, Wilson KS, Vorgias CE. 1994. Crystal structure of a bacterial chitinase at 2.3 Å resolution. *Structure 2*:1169–1180.

Pomes R, Roux B. 1995. Structure and dynamics of a proton wire: A theoretical study of the gramicidin channel. *Biophys J 68*:A150.

Qi PX, DiStefano DL, Wand AJ. 1994a. Solution structure of horse heart ferrocytochrome *c* determined by high resolution NMR and restrained simulated annealing. *Biochemistry 33*:6408–6417.

Qi PX, Urbauer JL, Fuentes EJ, Leopold MF, Wand AJ. 1994b. Structural water in oxidized and reduced horse heart cytochrome *c*. *Nature Struct Biol 1*:378–382.

Rasmussen BF, Stock AM, Ringe D, Petsko GA. 1992. Crystalline ribonuclease A loses function below the dynamical transition at 220 K. *Nature 357*:423–424.

Rich PR, Bendall DS. 1980. The redox potentials of the *b*-type cytochromes of higher plant chloroplasts. *Biochim Biophys Acta 591*:153–161.

Rongey SH, Paddock ML, Feher G, Okamura MY. 1993. Pathway of proton transfer in bacterial reaction centers: Second-site mutation Asn-M44 → Asn mutant of *Rhodobacter sphaeroides*. *Proc Natl Acad Sci USA 90*:1325–1329.

Rottenberg H, Grunwald T. 1973. Determination of ΔpH in chloroplasts. *Eur J Biochem 25*:71–74.

Roux B, Prod'hom B, Karplus M. 1995. Ion transport in the gramicidin channel: Molecular dynamics study of single and double occupancy. *Biophys J 68*:876–892.

Sundberg RJ, Gupta G. 1973. Nitrogen-carbon linkage isomerism of histidine in ruthenium ammine complexes. *Bioinorganic Chem 3*:39–48.

Takahashi E, Wraight CA. 1990. A crucial role for Asp^{L213} in the proton transfer pathway to the secondary quinone of reaction centers from *Rhodobacter sphaeroides*. *Biochim Biophys Acta 1020*:107–111.

Takahashi E, Wraight CA. 1992. Proton and electron transfer in the acceptor quinone complex of *Rhodobacter sphaeroides* reaction centers: Characterization of site-directed mutants of the two ionizable residues, Glu^{L212} and Asp^{L213}, in the Q_B binding site. *Biochemistry 31*:855–866.

Wikström MKF, Krab K, Saraste M. 1981. *Cytochrome oxidase: A synthesis*. New York: Academic Press. Chapter 7.

Williams MA, Goodfellow JM, Thornton JM. 1994. Buried waters and internal cavities in monomeric proteins. *Protein Sci 3*:1224–1235.

Yagil G. 1967. The proton dissociation constant of pyrrole, indole and related compounds. *Tetrahedron 23*:2855–2861.